

UCLA

UCLA Previously Published Works

Title

Costimulation-adhesion blockade is superior to Cyclosporine A and prednisone immunosuppressive therapy for preventing rejection of differentiated human embryonic stem cells following transplantation

Permalink

<https://escholarship.org/uc/item/9nd270kj>

Journal

Stem Cells, 31(11)

ISSN

1066-5099

Authors

Huber, Bruno C
Ransohoff, Julia D
Ransohoff, Katherine J
et al.

Publication Date

2013-11-01

DOI

10.1002/stem.1501

Peer reviewed



Published in final edited form as:

Stem Cells. 2013 November ; 31(11): 2354–2363. doi:10.1002/stem.1501.

Costimulation-Adhesion Blockade is Superior to Cyclosporine A and Prednisone Immunosuppressive Therapy for Preventing Rejection of Differentiated Human Embryonic Stem Cells Following Transplantation

Bruno C. Huber^{1,2,*}, Julia D. Ransohoff^{1,2,3,*}, Katherine J. Ransohoff², Johannes Riegler^{1,2}, Antje Ebert^{1,2}, Kazuki Kodo^{1,2}, Yongquan Gong^{2,3}, Veronica Sanchez-Freire^{1,2}, Devaveena Dey^{1,2}, Nigel G. Kooreman^{1,2}, Sebastian Diecke^{1,2}, Wendy Y. Zhang^{1,2}, Justin Odegaard⁵, Shijun Hu^{1,2}, Joseph D. Gold^{1,3}, Robert C. Robbins³, and Joseph C. Wu^{1,2,4}

¹Stanford Cardiovascular Institute, Stanford University School of Medicine, Stanford, CA

²Departments of Medicine and Radiology, Stanford University School of Medicine, Stanford, CA

³Department of Cardiothoracic Surgery, Stanford University School of Medicine, Stanford, CA

⁴Institute of Stem Cell Biology and Regenerative Medicine, Stanford University School of Medicine, Stanford, CA

⁵Department of Pathology, Stanford University School of Medicine, Stanford, CA

Abstract

Rationale—Human embryonic stem cell (hESC) derivatives are attractive candidates for therapeutic use. The engraftment and survival of hESC derivatives as xenografts or allografts require effective immunosuppression to prevent immune cell infiltration and graft destruction.

Objective—To test the hypothesis that a short-course, dual-agent regimen of two costimulation-adhesion blockade agents can induce better engraftment of hESC derivatives compared to current immunosuppressive agents.

Methods and Results—We transduced hESCs with a double fusion reporter gene construct expressing firefly luciferase (Fluc) and enhanced green fluorescent protein (eGFP), and differentiated these cells to endothelial cells (hESC-ECs). Reporter gene expression enabled longitudinal assessment of cell engraftment by bioluminescence imaging (BLI). Costimulation-adhesion therapy resulted in superior hESC-EC and mouse EC engraftment compared to cyclosporine therapy in a hindlimb model. Costimulation-adhesion therapy also promoted robust hESC-EC and hESC-derived cardiomyocyte (hESC-CM) survival in an ischemic myocardial injury model. Improved hESC-EC engraftment had a cardioprotective effect after myocardial

Correspondence: Joseph C. Wu, MD, PhD, Lorry I. Lokey Stem Cell Research Building, 265 Campus Drive, Rm G1120B, Stanford, CA 94305-5454. Ph: 650-736-2246. Fax: 650-736-0234. joewu@stanford.edu.

*Both authors contributed equally to this work

DISCLOSURES

None.

AUTHOR CONTRIBUTIONS

Bruno C. Huber and Julia D. Ransohoff: Conception and design, data analysis and interpretation, manuscript writing, final approval of manuscript; Katherine J. Ransohoff, Johannes Riegler, Antje Ebert, Kazuki Kodo, Yongquan Gong, Veronica Sanchez-Freire, Devaveena Dey, Nigel G. Kooreman, Sebastian Diecke, Wendy Y. Zhang, Justin Odegaard, Shijun Hu: Collection and/or assembly of data, final approval of manuscript; Robert C. Robbins, Joseph D. Gold: Data analysis and interpretation, final approval of manuscript; Joseph C. Wu: Conception and design, financial support, manuscript writing, final approval of manuscript.

injury, as assessed by magnetic resonance imaging (MRI). Mechanistically, costimulation-adhesion therapy is associated with systemic and intra-graft upregulation of T cell immunoglobulin and mucin domain 3 (TIM3) and a reduced pro-inflammatory cytokine profile.

Conclusions—Costimulation-adhesion therapy is a superior alternative to current clinical immunosuppressive strategies for preventing the post-transplant rejection of hESC derivatives. By extending the window for cellular engraftment, costimulation-adhesion therapy enhances functional preservation following ischemic injury. This regimen may function through a TIM3-dependent mechanism.

Keywords

immune tolerance; costimulation blockade; immunosuppressive drugs; embryonic stem cells; endothelial cells; myocardial infarction

INTRODUCTION

Human embryonic stem cell (hESC) and induced pluripotent stem cell (iPSC) derivatives are attractive candidates for therapeutic use, with the potential to replace deficient cells and to improve functional recovery in injury or disease settings^{1, 2}. The therapeutic potential of these cells, however, may depend on their long-term survival following transplantation. Engraftment and survival of hESC-derived xenografts or allografts require effective immunosuppression to prevent immune cell infiltration and graft destruction³. Clinical transplantation regimens are systemically toxic and require chronic agent delivery, leaving the host immunocompromised and susceptible to infection⁴. The ideal therapeutic regimen would require only short-term agent delivery while promoting long-term graft survival.

However, investigators have yet to demonstrate optimal strategies to promote the long-term survival of hESC derivatives, which is hampered by a formidable immunologic barrier⁵. hESCs lack expression of major histocompatibility (MHC) class II molecules and express low levels of MHC class I molecules, both of which increase upon differentiation into specialized antigen-presenting cells⁶. Undifferentiated hESCs exhibit some level of immune privilege and immunosuppressive effects, which may be related to the tumor-like microenvironment created with *in vivo* differentiation⁷. Before moving pluripotent cell therapies to larger animal models and to the clinic, investigators need to establish methods that ensure the long-term survival of human differentiated stem cells in small animal models^{5, 8}. To this end, endothelial cells (ECs) hold clinical promise and have demonstrated success in various models. Several reports have now provided convincing evidence that endothelial cell transplantation promotes myocardial recovery through a variety of mechanisms, including but not limited to paracrine signaling⁹ and by supporting the spatial organization of host cardiomyocytes¹⁰.

T cell activation requires two signals, which result from (1) antigen-specific T cell receptor ligation and (2) non-antigen-specific costimulatory molecule signaling. The presence of signal (1) and absence of signal (2) prevents optimal T cell activation, resulting in the abortive activation or death of donor-reactive T cells, lowering the production of interleukin-2 (IL-2), and generating a state of T cell anergy¹¹. Here we test the hypothesis that a short-course regimen of two agents that results in costimulation-adhesion blockade delivered in four doses in the days following hESC-derived endothelial cell (hESC-EC) or hESC-derived cardiomyocyte (hESC-CM) transplantation can induce prolonged cell engraftment in intramuscular, subcutaneous, and/or intramyocardial murine models, and that this improved cell survival can also enhance the cardioprotective effect in an ischemic myocardial injury model.

MATERIALS AND METHODS

Study design

A schematic overview of the study is provided in Supplementary Figure 1. hESCs were transduced with a lentiviral Fluc-eGFP double fusion construct as previously described³. hESCs were differentiated into endothelial cells (hESC-ECs) or cardiomyocytes (hESC-CMs). Differentiated cells were transplanted into one of two models: (i) hindlimb injection or (ii) cardiac injection following ligation of the left anterior descending coronary artery (LAD). Costimulation-adhesion blockade therapy consisted of anti-LFA-1 (M17/4) and CTLA4-Ig (BioXCell, West Lebanon, NH) administered intraperitoneally (i.p.) at a dose of 20 mg/kg on days 0, 2, 4, and 6 after transplantation. For comparison with conventional immunosuppressive protocol, CsA (Novartis, New York, NY; 10 mg/kg/day, i.p.) and Prednisone (2 mg/kg/day, i.p.) were given daily.

(i) Hindlimb injection

Animals received 3×10^6 hESC-ECs or immortalized mouse ECs (Weill Cornell Medical College, New York, NY), which were transfected with SV40 T antigen and human telomerase by lentiviral vectors, and which exhibit stable EC phenotype. We transplanted both xenogeneic (i.e., hESC-ECs) and allogeneic (i.e., mouse ECs) cells, as previously described³, to allow for comparison of survival in these settings. Animals were randomized into the following groups: (1) hESC-ECs with costimulation-adhesion therapy (hESC-ECs + costim; n=15); (2) hESC-ECs with CsA and prednisone (hESC-ECs + CsA/Pred; n=15); (3) hESC-ECs without therapy (hESC-ECs + no treatment; n=15); (4) immunodeficient animals (SCID, n=15; Nude, n=5; NSG, n=5); (5) Mouse ECs with costimulation-adhesion therapy (n=10); (6) Mouse ECs with no therapy (n=10); and (7) Mouse ECs with costimulation-adhesion therapy + sirolimus (n=10, Wyeth Pharmaceuticals, Madison, NJ) at 1.5 ug/dose as previously described¹². Cell survival was monitored by optical bioluminescence imaging (BLI) on days 2, 4, 7, 10, 14, 21, 28, and 35. Harvested and cultured tissues were analyzed *ex vivo* by fluorescent activated cell sorting (FACS), RT-PCR, and Luminex cytokine profiling.

(ii) Myocardial infarction (MI) model

We transplanted 2×10^6 hESC-ECs or 2×10^6 hESC-CMs into the ischemic myocardium following ligation of the left anterior descending (LAD) coronary artery, in order to compare survival of these cell types. Animals were randomized into the following groups: (1) hESC-ECs + costimulation-adhesion (n=15); (2) hESC-ECs + CsA/Pred (n=15); (3) hESC-ECs + no treatment (n=15); (4) no cells + costimulation-adhesion (n=15); (5) no cells + PBS (n=15); (6) hESC-CMs + costimulation-adhesion (n=5); (7) hESC-CMs + CsA/Pred (n=5); and (8) hESC-CMs + no treatment (n=5). Cell survival was monitored by BLI on days 2, 4, 7, 10, 14, 21, 28, and 35. Cardiac function was assessed by magnetic resonance imaging (MRI) on days 2 and 28 post-MI (groups 1–5). Histological analysis was performed on hearts from randomly selected animals at 4 weeks post-infarction. Cell survival was monitored by BLI on days 2, 4, 7, 10, 14, 21, 28, and 35 post-MI.

Characterization of hESC-ECs

Undifferentiated hESCs (H9 line; obtained from WiCell, Madison, WI) were grown and expanded on Matrigel-coated plates in mTeSR1 medium (Stem Cell Technologies, Vancouver, BC, Canada) as previously described¹³. To confirm the pluripotent state of hESCs, quantitative polymerase chain reaction (q-PCR) analysis demonstrating the expression of key transcription factors associated with pluripotency and *in vivo* teratoma formation assays were performed, as described previously⁹ and as further detailed in the

Supplementary Methods section. hESCs were differentiated to hESC-ECs, as outlined in Figure 1A, and as previously described¹⁴. For further details of the differentiation protocol, please refer to the Supplementary Methods section. hESC-ECs were subjected to *in vitro* hypoxic conditions to profile their paracrine signaling and growth factor release.

Characterization of hESC-CMs

Undifferentiated hESCs (H7 line; obtained from WiCell, Madison, WI) were grown and expanded on Matrigel-coated plates in mTeSR1 medium (Stem Cell Technologies, Vancouver, BC, Canada) as previously described¹³. At 90% confluence, hESCs were subsequently differentiated into beating cardiomyocytes using a small molecule-based monolayer method adapted after Lian et al.¹⁵ and described in detail by Hu et al¹⁴.

Animal surgery and cell transplantation

Myocardial infarction (MI) was induced in immunocompetent FVB and immunodeficient NOD/SCID mice (Charles River Laboratories, Wilmington, MA) by LAD ligation under 1.5% to 2% inhaled isoflurane anesthesia. Cell and PBS injections were performed at 2 sites on the anterolateral wall with a total volume of 30 μ l using a 29-gauge Hamilton syringe immediately following injury. All operations were performed by a blinded microsurgeon (Y.G.). For the hindlimb model, cells were injected unilaterally or bilaterally into the gastrocnemius muscles of C57BL/6J, Nude, NSG, or SCID mice in 50 μ l Matrigel (BD) using a 29-gauge Hamilton syringe, and animals randomized to the costim-adhesion therapy group received these agents at days 0, 2, 4, and 6 post-cell transplantation. Study protocols were approved by the Stanford Animal Research Committee. Animal care was provided in accordance with the Stanford University School of Medicine guidelines and policies for the use of laboratory animals.

Bioluminescence imaging (BLI) of cell transplantation

BLI (n=8–10/group) was performed on all animals that survived surgical procedures using the Xenogen In Vivo Imaging System (PerkinElmer, Waltham, MA) as previously described¹⁶ and detailed in the Supplementary Methods section.

Cardiac magnetic resonance imaging (MRI)

For evaluation of myocardial function, mice (n=6–9/group) were imaged on days 2 and 28 post-MI using a 7T MR901 Discovery horizontal bore scanner (Agilent Technologies, Santa Clara, CA) with a shielded gradient system (600 mT/m). Short- and long-axis images for each animal were combined into one dataset, randomized, and made anonymous. Images were analyzed as previously described¹⁷ using the cardiac analysis software Segment (<http://segment.heiberg.se>). Additional details are provided in the Supplementary Methods section.

Immunofluorescence staining and confocal microscopy

Primary antibodies against human CD31 (Invitrogen, Carlsbad, CA), laminin (Abcam, Cambridge, MA), CD144 (BD, San Jose, CA), cardiac troponin T (Thermo Fisher Scientific, Waltham, MA and Abcam), and sarcomeric alpha-actinin (Sigma, St. Louis, MO) and secondary antibodies (goat anti-mouse Alexa Fluor 488 and goat anti-rabbit Alexa Fluor 594) were used. Briefly, endothelial cells growing on gelatin-coated 12 mm glass coverslips were fixed in 4% PFA. Cells were blocked with 1% BSA for 1 hr at room temperature, followed by addition of the primary antibody at a dilution of 1:100 for 2 hr at room temperature. Secondary antibody was added at a dilution of 1:100 for 1 hr at room temperature. Cardiomyocyte stainings were performed following a previously described protocol¹⁸. Primary and secondary antibodies were added in 1% BSA and 0.1% Triton X-100 to individually stained coverslips. Pictures were taken with 10x, 20x, and 40x plan

apochromat, and 63x plan apochromat (oil) objectives using a confocal microscope (Carl Zeiss, LSM 510 Meta, Göttingen, Germany) and ZEN software (Carl Zeiss).

Quantitative gene expression analysis

Please refer to the Supplementary Methods section.

Flow cytometry analysis

Please refer to the Supplementary Methods section.

T cell activation and mouse cytokine array

Please refer to the Supplementary Methods section.

Statistical analysis

Experimental results are expressed as mean \pm SEM. Linear regression analysis was performed to determine the correlation between 2 variables. ANOVA and repeated measures ANOVA with post-hoc testing as well as the 2-tailed Student t test were used. Differences were considered significant at probability values of 0.05.

RESULTS

Costimulation-adhesion blockade is superior to cyclosporine therapy in promoting engraftment of transplanted hESC-ECs

To generate a therapeutically relevant cell population, undifferentiated hESCs were differentiated to endothelial cells (hESC-ECs) using a differentiation protocol consisting of activin A, BMP4, FGFb, and VEGF-A (Figure 1A). The undifferentiated parental line readily proliferates (Figures S2A–B) and forms teratomas (Figure S2C) in immunodeficient hosts. To confirm successful differentiation to endothelial cells, we performed confocal microscopy and observed appropriate expression of CD31, CD144, and laminin (Figure 1B). To test endothelial cell marker expression at the gene expression level, we performed RT-PCR and observed robust expression of CD31 and CD144 compared to undifferentiated hESCs and fibroblasts, and downregulated expression of Oct4, Sox2, and Nanog (Figure 1C), markers associated with pluripotency. As expected, hESC-ECs readily took up DiI-ac-LDL (Figure 1D) while undifferentiated hESCs did not take up the substrate, and neither hESC-ECs nor hESCs exhibited autofluorescence in the absence of the probe (Figure S2D). As expected, hESC-ECs formed tubules in a tube formation assay (Figure 1E), whereas undifferentiated hESCs did not form tubular structures (Figure S2E).

Prior to differentiation, hESCs were transduced with a double fusion reporter gene construct expressing Fluc and enhanced eGFP to enable *in vivo* tracking of transplanted cells¹⁹ (Figure 2A). Cell count is robustly correlated with Fluc signal ($R^2 = 0.99$) (Figures 2B–C). We first transplanted hESC-ECs into hindlimbs of immunodeficient and immunocompetent mice. Immunodeficient NOD scid gamma (NSG) mice lack functional natural killer cells, but Nude mice retain functional natural killer cells; both lack mature T- and B-lymphocytes²⁰. We observed robust graft survival in both immunodeficient strains up to 28 days post-transplantation (Figures 2D–E) ($p = \text{NS}$, NSG compared to Nude).

We next tested various immunosuppressive therapies (Figure 3A) to promote cell engraftment in immunocompetent hosts. Cyclosporine (CsA), one of the primary clinical immunosuppressive agents used following cardiac transplantation, has been used extensively in human cell xenotransplantation models of cardiac repair (reviewed elsewhere²¹). None of the studies using CsA, to our knowledge, have longitudinally

assessed graft survival by *in vivo* imaging, relying instead on histological or functional outcomes²¹. Therefore, we used BLI to assess chronic CsA and prednisone therapy, and we found that they did not significantly prolong hESC-EC survival compared to no immunosuppression, with graft rejection by day 10 (Figures 3B–C) ($p = \text{NS}$). By contrast, short-term administration of CTLA4-Ig and anti-LFA-1 (costimulation-adhesion) permitted the long-term engraftment of hESC-ECs ($p < 0.05$) (Figures 3D–E and Figure S3A). Because successful immunosuppressive approaches have broad clinical potential with respect to host tissues or graft delivery sites, we also delivered hESC-ECs in a subcutaneous Matrigel plug matrix, and observed similar patterns of cell graft survival as those seen in the hindlimb injection model, with superior survival in immunodeficient compared to immunocompetent hosts (Figures S3B–C) ($p < 0.05$), and superior results from costimulation-adhesion compared to CsA and prednisone therapy ($p < 0.05$) (Figures S3D–E). Neither the addition of prednisone (Figures S3D–E) nor of sirolimus (Figure S4A), which acts independently of costimulatory molecule signaling⁴, to the costimulation-adhesion regimen significantly improved its efficacy. Costimulation-adhesion therapy also promoted the superior engraftment of allogeneic immortalized mouse endothelial cells ($p < 0.05$) (Figures S4B–C) and resulted in enhanced graft size (Figure S4D).

Costimulation-adhesion blockade mitigates immunological rejection of hESC-ECs and hESC-CMs after transplantation into the ischemic myocardium

After establishing the superiority of costimulation-adhesion therapy in a non-ischemic model, we next investigated whether this regimen could promote the engraftment of hESC-ECs in ischemic hindlimb and acute myocardial infarction (MI) models. In the ischemic hindlimb model, hESC-EC survival was limited to day 10 post-transplantation, whereas costimulation-adhesion therapy significantly improved cell engraftment beyond two weeks post-transplantation in the ischemic setting (Figures S5A–B). In the MI model, hESC-ECs were rejected in immunocompetent animals by day 10, whereas hESC-ECs engrafted in immunodeficient SCID mice up to 21 days post-transplantation (Figures 4A–B) ($p < 0.05$). Similar to the non-ischemic hindlimb model (see Figures 3B–E), CsA and prednisone therapy did not improve graft survival after MI compared to costimulation-adhesion therapy ($p < 0.05$); costimulation-adhesion therapy again permitted superior graft survival compared to that observed in immunocompetent animals (Figures 4C–D) ($p < 0.05$). BLI signal was $10,481 \pm 3,087$ photons/sec/cm²/sr in costimulation-adhesion-treated animals at two weeks post-transplantation, and $4,718 \pm 498$ photons/sec/cm²/sr in CsA-treated animals ($p < 0.05$). By day 35 post-transplantation, BLI signal did not differ significantly from day 14 in costimulation-adhesion-treated animals ($9,673 \pm 2,925$ photons/sec/cm²/sr; $p = \text{NS}$), but was significantly lower in CsA-treated animals compared to signal at day 14 ($3,560 \pm 80$ photons/sec/cm²/sr; $p < 0.05$).

In order to investigate whether the efficacy of costim-adhesion therapy is limited to promoting the survival of hESC-ECs, we also transplanted another differentiated cell type (i.e., hESC-CMs) into the ischemic myocardium. Prior to transplantation, we characterized hESC-CMs. Gene expression profiling of hESC-CMs revealed upregulation of cardiac genes including TNNT2, MYH6, and MYL2 compared to undifferentiated hESCs (Figure S6A) as well as positive expression of sarcomeric proteins (α -sarcomeric actinin and Troponin T) and connexin-43 (Figure S6B). Following transplantation into the ischemic myocardium, we monitored graft preservation by BLI in animals receiving costimulation-adhesion therapy, CsA and prednisone therapy, or no treatment. As with the transplantation of hESC-ECs, we observed the superior engraftment of hESC-CMs in costimulation-adhesion-treated hosts compared to CsA and prednisone-treated hosts as well as control animals (Figure S6C–D; $p < 0.05$).

Improved cell survival is correlated with functional protection in the MI model

It has been suggested in previous studies that cell engraftment is not necessary for therapeutic benefits. To test the hypothesis that long-term graft survival would result in superior benefits, we performed cardiac MRI following MI in immunocompetent mice randomized to receive: (1) hESC-ECs + costimulation-adhesion therapy; (2) hESC-ECs + CsA and prednisone therapy; (3) hESC-ECs + no treatment; (4) no cells + costimulation-adhesion therapy; or (5) no cells + PBS. Following confirmation of MI by myocardial blanching and ECG changes (Figures S7A–B), we observed significant preservation of cardiac function, including increased left ventricular ejection fraction (EF), decreased end diastolic volumes (EDV), and decreased end systolic volumes (ESV) in animals receiving hESC-ECs with costimulation-adhesion therapy compared to all other groups (Figures 5A–E, S8, and Supplementary Table 1; ANOVA, $p < 0.05$). Furthermore, we qualitatively observed attenuated cardiac remodeling in animals receiving hESC-ECs and costimulation-adhesion therapy compared to controls. Histological analysis also revealed smaller infarct size and decreased left ventricular wall thinning (Figures S9A–D).

To investigate why transplanted hESC-ECs may promote functional recovery, we profiled paracrine signaling by hESC-ECs *in vitro* under hypoxic conditions analogous to those of the ischemic myocardium. We observed that, under low oxygen conditions, hESC-ECs expressed higher levels of VEGF-A, IL-1 α , FGF1, TNF- α , and TGF- α as well as lower levels of TIMP1 and TIMP2 than when they were under normoxic conditions, which may functionally contribute to their role in promoting neoangiogenesis in an ischemic transplantation setting (Figure S10).

Superior cell engraftment by costimulation-adhesion blockade is correlated with upregulation of TIM3 and downregulation of pro-inflammatory cytokine profile

To better understand the mechanism by which costimulation-adhesion therapy promotes cell engraftment, we profiled cell surface marker expression on splenocytes isolated from treated and control animals, and on hESC-EC-implanted gastrocnemius muscles. We found a marked increase in the percentage of TIM3⁺PD1⁺ cells in the splenocytes (Figures 6A–B) and of TIM3⁺ cells in muscles (Figures 6C–D) of treated animals. Gene expression analysis of lymph nodes revealed similarly upregulated TIM3 and PD1 expression in treated animals (Figures 6E–F). In profiling splenocyte cytokine levels after stimulating cells with phorbol 12-myristate 13-acetate (PMA) and ionomycin, we found important differences between treated and untreated hosts (Supplementary Table 2). In particular, we observed a reduced pro-inflammatory cytokine profile in costimulation-adhesion-treated animals. Notably, our data showed significantly decreased IL-2 levels in costimulation-adhesion-treated animals, as well as decreased interferon- γ (IFN- γ) and macrophage inflammatory protein-1 α (MIP1- α), and increased interleukin-4 (IL-4) levels, although the changes in the latter three did not reach statistical significance (Figures 6G–J).

DISCUSSION

The immunogenicity of stem cell-based grafts presents a significant barrier to successful regenerative therapies⁵. The requirement to demonstrate efficacy and safety of human stem cell-derived therapies in animal models adds an additional level of complexity, because xenograft rejection is difficult to overcome. Previous investigations have provided strong evidence supporting the ability of costimulation-adhesion blockade therapy to promote the long-term engraftment of undifferentiated murine and human pluripotent cells³. However, because of their potential for tumorigenicity²², future clinical studies incorporating pluripotent stem cell therapies are expected to use these cells' derivatives instead.

Here we describe a short-course immunosuppressive strategy to promote the engraftment of hESC-ECs compared to current clinical immunosuppressive agents. The major findings can be summarized as follows: (1) Costimulation-adhesion therapy resulted in superior mouse EC and hESC-EC engraftment compared to Cyclosporine A and prednisone therapy in a hindlimb model; (2) Costimulation-adhesion therapy promoted robust hESC-EC and hESC-CM survival in the ischemic myocardium; (3) Improved hESC-EC engraftment after costimulation-adhesion treatment resulted in a cardioprotective effect following myocardial infarction as assessed by MRI; and (4) mechanistically, costimulation-adhesion therapy is associated with systemic and intra-graft upregulation of TIM3 and a reduced pro-inflammatory cytokine profile.

This simple and effective regimen entails the brief administration of CTLA4-Ig and anti-LFA-1. CTLA4-Ig binds CD80 and CD86 (B7-1 and -2); this binding outcompetes CD28 for engagement with CD80 and CD86, an interaction important for T cell stimulation²³. Anti-LFA-1 blocks the interaction of LFA-1, a β 2 integrin, with its receptor, ICAM-1; this interaction prevents delivery of a costimulatory signal involved in the activation of resting T cells²⁴, and prevents optimal T-cell priming in the immunological synapse²⁵. Previous investigations have demonstrated the efficacy of a tri-agent regimen in prolonging the survival of undifferentiated stem cells, but not of their derivatives; these investigations have also demonstrated that no single agent used as monotherapy prolonged graft survival beyond two weeks post-transplantation³. The derivatives of pluripotent stem cells are more immunogenic than their undifferentiated parental lines, so we reasoned that multiple agents would be required to promote the long-term survival of ESC derivatives. However, the aforementioned tri-agent regimen required the use of a monoclonal antibody against CD154 (CD40L), which has not been pursued clinically since the halting of its phase I clinical trial testing in non-human primates due to thromboembolic events²⁶, so we sought to devise a successful regimen excluding its use. All clinically feasible immunosuppressive approaches must address the important issue of agent-induced side effects. Abatacept and belatacept, clinical correlates of the CTLA4-Ig fusion protein tested in this study, are FDA-approved for use following renal transplantation and for the treatment of rheumatoid arthritis^{25,27}. In addition to efalizumab, an antibody against LFA-1, a new class of anti-adhesion molecule agents is being pursued clinically. Anti-VLA4 therapy is FDA-approved for treating multiple sclerosis, and is under active investigation for its promising role as a post-transplantation immunosuppressive agent⁸.

While CsA and steroid therapy has well-documented pathological associations with hypertension, hyperlipidemia, infection, increased malignancy risk, hepatotoxicity, and nephrotoxicity, as well significant side effects such as gingival hyperplasia and hypertrichosis²⁸, costimulation-adhesion blockade therapy results in no statistically significant alterations in complete blood count with manual differential, chemistry, and electrolyte panels³. Given its extensive use in laboratory and clinical settings, we were surprised by CsA's inability to permit significant long-term cell survival. While bioluminescent imaging (BLI) can, in theory, detect photon emission from single, live cell populations, there are practical limitations to its sensitivity. For example, light transmission from viable cells is subject to signal attenuation and emission scatter related to tissue depth²⁹. To our knowledge, no other studies have used BLI to profile the kinetics of graft destruction under a CsA and steroid regimen; others have reported graft preservation by positive histological stains at several weeks post-transplantation, or by improvement in cardiac function with cell therapy²¹. Therefore, we interpret our lack of persistent BLI signal in CsA-treated hosts as indicative of significant, but not necessarily complete, graft destruction.

Interestingly, our data show that costimulation-adhesion blockade is correlated with the marked upregulation of TIM3 on splenocytes, on cells infiltrating muscle tissue implanted with hESC-ECs, and on lymph node cells of treated hosts, suggesting that costimulation-adhesion blockade may induce inhibitory molecules associated with T cell exhaustion³⁰. CsA is a calcineurin inhibitor that, through downstream action, results in decreased activation of IL-2; sirolimus is an mTOR inhibitor that prevents the activation of IL-2; costimulation-adhesion therapy indirectly reduces IL-2 levels following *ex vivo* PMA and ionomycin stimulation. The increased IL-4 and decreased IFN- γ levels we observed in costimulation-adhesion-treated animals are consistent with downregulated humoral and cellular immune pathways, as IL-4 produced by T-helper-2 (T_H2) cells stimulates humoral immunity and IFN- γ produced by T-helper-1 (T_H1) cells activates cellular immunity⁴. We observed stronger cell engraftment in immunocompetent animals treated with costimulation-adhesion therapy than in immunodeficient SCID hosts, which retain some innate immune function, indicating that our regimen may depress both adaptive and innate immunity.

While the literature is replete with reports of TIM3 expression in HIV infection³¹ and of anti-TIM3 therapies for inducing anti-tumor immunity³², there are far fewer reports on the role of TIM3 in transplant immunology. TIM3 is expressed *in vivo* by IFN- γ -secreting T_H1 cells, dendritic cells, monocytes, and subsets of CD4⁺ and CD8⁺ T cells³³. It has been previously reported that TIM3 pathway blockade prevents the ability of costimulation-adhesion blockade agents to induce tolerance to MHC-mismatched allografts³⁴, and that TIM3 upregulation on tumor-specific CD8⁺ T cells causes T cell dysfunction³⁵. TIM3 expression on activated T_H1 cells is mirrored by TIM3 ligand expression on CD4⁺ regulatory T cells³⁶, which can exhibit donor-specific immunoregulatory and immunosuppressive effects *in vivo* by promoting self-tolerance³⁷ and allogeneic graft acceptance³⁸. Interestingly, the interaction of TIM3 with its ligand is necessary for donor-specific CD4⁺CD25⁺ regulatory T cell generation, but not for its function³⁴. These data suggest that further work is needed to understand the role of costimulation-adhesion blockade agents in regulatory T cell production and the potential role of TIM3. If targeted abrogation of TIM3 expression on T cells in combination with costimulation-adhesion therapy and hESC-derivative transplantation can induce more rapid graft rejection, TIM3 may play a critical role in regulating T cell graft-directed activity. Further work using transgenic mouse models or pharmacological TIM3-inhibition may clarify whether the relationship between TIM3 expression and costimulation-adhesion therapy is correlational or potentially causal.

This study also makes the important observation that significantly improved cardiac function as assessed by longitudinal MRI requires both cell transplantation and effective immunosuppression. We did not observe any functional improvement in animals that rapidly rejected cell grafts in the absence of adequate immunosuppression. This suggests that graft preservation is required for therapeutic benefit; in addition to their potential to participate directly in new vessel formation, long-lived cells may act as cytokine delivery vehicles or activators of paracrine signaling to promote recovery in the ischemic environment³⁹. Furthermore, these data indicate that successful stem cell based therapies may require the reliable engraftment of a sufficient number of transplanted cells.

CONCLUSION

In summary, this study demonstrates that a short course of costimulation-adhesion blockade treatment is sufficient to induce engraftment of xenogeneically transplanted hESC derivatives in both injured and healthy tissues, and to promote cardiac protection. Costimulation-adhesion therapy is associated with systemic and intra-graft upregulation of TIM3 and a reduced pro-inflammatory cytokine profile. The transplantation of hESC and

iPSC derivatives holds great therapeutic promise, with clinical trials on the immediate horizon^{40,41}. This study represents an important step forward in overcoming the immunologic barriers that have continued to hamper the full realization of highly promising pluripotent stem cell-based therapies⁴², and that must be addressed before their eventual clinical application.

Supplementary Material

Refer to Web version on PubMed Central for supplementary material.

Acknowledgments

This work was supported by research grants from the Deutsche Forschungsgemeinschaft (BCH, AE, and SD), the Austrian Science Fund (JR), NIH U01 HL099776, NIH AI085575, NIH EB009689, Leducq Foundation, Burroughs Wellcome Foundation, and California Institute of Regenerative Medicine DR2-05394 and TR3-05556 (JCW).

References

1. Passier R, van Laake LW, Mummery CL. Stem-cell-based therapy and lessons from the heart. *Nature*. 2008; 453:322–329. [PubMed: 18480813]
2. BurrIDGE PW, Keller G, Gold JD, et al. Production of de novo cardiomyocytes: human pluripotent stem cell differentiation and direct reprogramming. *Cell Stem Cell*. 2012; 10:16–28. [PubMed: 22226352]
3. Pearl JI, Lee AS, Leveson-Gower DB, et al. Short-term immunosuppression promotes engraftment of embryonic and induced pluripotent stem cells. *Cell Stem Cell*. 2011; 8:309–317. [PubMed: 21362570]
4. Swijnenburg RJ, Schrepfer S, Govaert JA, et al. Immunosuppressive therapy mitigates immunological rejection of human embryonic stem cell xenografts. *Proc Natl Acad Sci U S A*. 2008; 105:12991–12996. [PubMed: 18728188]
5. Okita K, Nagata N, Yamanaka S. Immunogenicity of induced pluripotent stem cells. *Circ Res*. 2011; 109:720–721. [PubMed: 21921270]
6. Swijnenburg RJ, Tanaka M, Vogel H, et al. Embryonic stem cell immunogenicity increases upon differentiation after transplantation into ischemic myocardium. *Circulation*. 2005; 112:1166–172. [PubMed: 16159810]
7. Koch CA, Gerald P, Platt JL. Immunosuppression by embryonic stem cells. *Stem Cells*. 2008; 26:89–98. [PubMed: 17962705]
8. Pearl JI, Kean LS, Davis MM, et al. Pluripotent stem cells: immune to the immune system? *Sci Transl Med*. 2012; 4:164ps125.
9. Gu M, Nguyen PK, Lee AS, et al. Microfluidic single-cell analysis shows that porcine induced pluripotent stem cell-derived endothelial cells improve myocardial function by paracrine activation. *Circ Res*. 2012; 111:882–893. [PubMed: 22821929]
10. Narmoneva DA, Vukmirovic R, Davis ME, et al. Endothelial cells promote cardiac myocyte survival and spatial reorganization: implications for cardiac regeneration. *Circulation*. 2004; 110:962–968. [PubMed: 15302801]
11. Wood KJ, Sakaguchi S. Regulatory T cells in transplantation tolerance. *Nat Rev Immunol*. 2003; 3:199–210. [PubMed: 12658268]
12. Ferrer IR, Wagener ME, Robertson JM, et al. Cutting edge: Rapamycin augments pathogen-specific but not graft-reactive CD8+ T cell responses. *J Immunol*. 2010; 185:2004–2008. [PubMed: 20631309]
13. Ludwig TE, Levenstein ME, Jones JM, et al. Derivation of human embryonic stem cells in defined conditions. *Nat Biotechnol*. 2006; 24:185–187. [PubMed: 16388305]
14. Hu S, Wilson KD, Ghosh Z, et al. MicroRNA-302 Increases Reprogramming Efficiency via Repression of NR2F2. *Stem Cells*. 2013; 31:259–268. [PubMed: 23136034]

15. Lian X, Hsiao C, Wilson G, et al. Robust cardiomyocyte differentiation from human pluripotent stem cells via temporal modulation of canonical Wnt signaling. *Proc Natl Acad Sci U S A*. 2012; 109:E1848–1857. [PubMed: 22645348]
16. Sheikh AY, Huber BC, Narsinh KH, et al. In vivo functional and transcriptional profiling of bone marrow stem cells after transplantation into ischemic myocardium. *Arterioscler Thromb Vasc Biol*. 2012; 32:92–102. [PubMed: 22034515]
17. Riegler J, Cheung KK, Man YF, et al. Comparison of segmentation methods for MRI measurement of cardiac function in rats. *J Magn Reson Imaging*. 2010; 32:869–877. [PubMed: 20882617]
18. Zhang J, Wilson GF, Soerens AG, et al. Functional cardiomyocytes derived from human induced pluripotent stem cells. *Circ Res*. 2009; 104:e30–41. [PubMed: 19213953]
19. Fluck N, Witzke O, Morris PJ, et al. Indirect allorecognition is involved in both acute and chronic allograft rejection. *Transplant Proc*. 1999; 31:842–843. [PubMed: 10083366]
20. Meyerrose TE, Herrbrich P, Hess DA, et al. Immune-deficient mouse models for analysis of human stem cells. *Biotechniques*. 2003; 35:1262–1272. [PubMed: 14682062]
21. Xiao YF, Min JY, Morgan JP. Immunosuppression and xenotransplantation of cells for cardiac repair. *Ann Thorac Surg*. 2004; 77:737–744. [PubMed: 14759483]
22. Lee AS, Tang C, Rao MS, et al. Tumorigenicity as a clinical hurdle for pluripotent stem cell therapies. *Nat Medicine*. 2013;9. in press.
23. Thompson CB, Allison JP. The emerging role of CTLA-4 as an immune attenuator. *Immunity*. 1997; 7:445–450. [PubMed: 9354465]
24. Nicolls MR, Coulombe M, Yang H, et al. Anti-LFA-1 therapy induces long-term islet allograft acceptance in the absence of IFN-gamma or IL-4. *J Immunol*. 2000; 164:3627–3634. [PubMed: 10725719]
25. Ford ML, Larsen CP. Translating costimulation blockade to the clinic: lessons learned from three pathways. *Immunol Rev*. 2009; 229:294–306. [PubMed: 19426229]
26. Kawai T, Andrews D, Colvin RB, et al. Thromboembolic complications after treatment with monoclonal antibody against CD40 ligand. *Nat Med*. 2000; 6:114.
27. Curtis JR, Singh JA. Use of biologics in rheumatoid arthritis: current and emerging paradigms of care. *Clin Ther*. 2011; 33:679–707. [PubMed: 21704234]
28. Patel JK, Kobashigawa JA. Cardiac transplant experience with cyclosporine. *Transplant Proc*. 2004; 36:323S–330S. [PubMed: 15041362]
29. Ransohoff JD, Wu JC. Imaging stem cell therapy for the treatment of peripheral arterial disease. *Curr Vasc Pharmacol*. 2012; 10:361–373. [PubMed: 22239638]
30. Stegagno M, Boyle LA, Preffer FI, et al. Functional analysis of T cell subsets and clones in human renal allograft rejection. *Transplant Proc*. 1987; 19:394–397. [PubMed: 3493557]
31. Jones RB, Ndhlovu LC, Barbour JD, et al. Tim-3 expression defines a novel population of dysfunctional T cells with highly elevated frequencies in progressive HIV-1 infection. *J Exp Med*. 2008; 205:2763–2779. [PubMed: 19001139]
32. Dardalhon V, Anderson AC, Karman J, et al. Tim-3/galectin-9 pathway: regulation of Th1 immunity through promotion of CD11b+Ly-6G+ myeloid cells. *J Immunol*. 2010; 185:1383–1392. [PubMed: 20574007]
33. Freeman GJ, Casanova JM, Umetsu DT, et al. TIM genes: a family of cell surface phosphatidylserine receptors that regulate innate and adaptive immunity. *Immunol Rev*. 2010; 235:172–189. [PubMed: 20536563]
34. Sanchez-Fueyo A, Tian J, Picarella D, et al. Tim-3 inhibits T helper type 1-mediated auto- and alloimmune responses and promotes immunological tolerance. *Nat Immunol*. 2003; 4:1093–1101. [PubMed: 14556005]
35. Fourcade J, Sun Z, Benallaoua M, et al. Upregulation of Tim-3 and PD-1 expression is associated with tumor antigen-specific CD8+ T cell dysfunction in melanoma patients. *J Exp Med*. 2010; 207:2175–2186. [PubMed: 20819923]
36. Monney L, Sabatos CA, Gaglia JL, et al. Th1-specific cell surface protein Tim-3 regulates macrophage activation and severity of an autoimmune disease. *Nature*. 2002; 415:536–541. [PubMed: 11823861]

37. Sakaguchi S, Sakaguchi N. Thymus and autoimmunity: capacity of the normal thymus to produce pathogenic self-reactive T cells and conditions required for their induction of autoimmune disease. *J Exp Med.* 1990; 172:537–545. [PubMed: 2373992]
38. Kingsley CI, Karim M, Bushell AR, et al. CD25+CD4+ regulatory T cells prevent graft rejection: CTLA-4- and IL-10-dependent immunoregulation of alloresponses. *J Immunol.* 2002; 168:1080–1086. [PubMed: 11801641]
39. Mirosou M, Jayawardena TM, Schmeckpeper J, et al. Paracrine mechanisms of stem cell reparative and regenerative actions in the heart. *J Mol Cell Cardiol.* 2011; 50:280–289. [PubMed: 20727900]
40. Schwartz SD, Hubschman JP, Heilwell G, et al. Embryonic stem cell trials for macular degeneration: a preliminary report. *Lancet.* 2012; 379:713–720. [PubMed: 22281388]
41. Garber K. Inducing translation. *Nat Biotechnol.* 2013; 31:483–486. [PubMed: 23752423]
42. de Almeida PE, Ransohoff JD, Nahid A, et al. Immunogenicity of pluripotent stem cells and their derivatives. *Circ Res.* 2013; 112:549–561. [PubMed: 23371903]

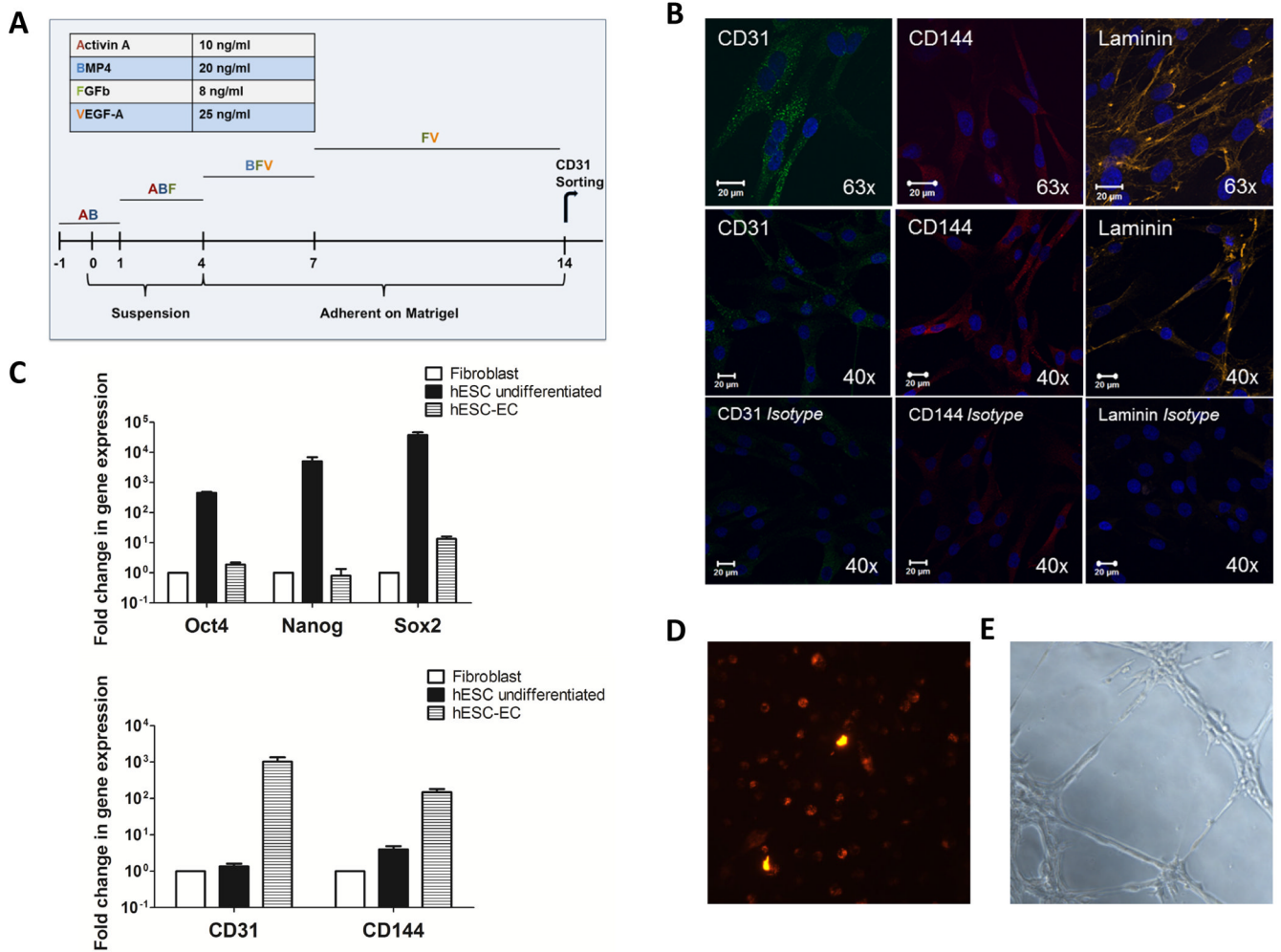


Figure 1.

Characterization of hESC-ECs. **(A)** Endothelial cell differentiation protocol.

Undifferentiated hESCs were grown on Matrigel and subcultured in low attachment dishes with differentiation medium supplement. At day 14, EBs in collagen were collected and digested and CD31⁺ cells were isolated by FACS and then sub-cultured in EGM-2 medium to expand.

(B) Expression of endothelial cell markers CD31, CD144, and Laminin by confocal microscopy. Cell nuclei stained with DAPI (blue). Scale bars = 20 μ m. **(C)** Gene expression profile (RT-PCR) of fibroblasts, undifferentiated ESCs, and hESC-ECS showing upregulation of CD31 and CD144 in hESC-ECs compared to undifferentiated hESCs and fibroblasts. Upregulation of pluripotency markers Sox2, Oct4, and Nanog is seen in undifferentiated hESCs compared to differentiated hESC-ECs and fibroblasts. Values were normalized to GAPDH and expression values are relative to fibroblasts. **(D)** hESC-ECs also can uptake ac-DiI-LDL and **(E)** form tube-like structures on Matrigel. Experiments were performed in triplicates.

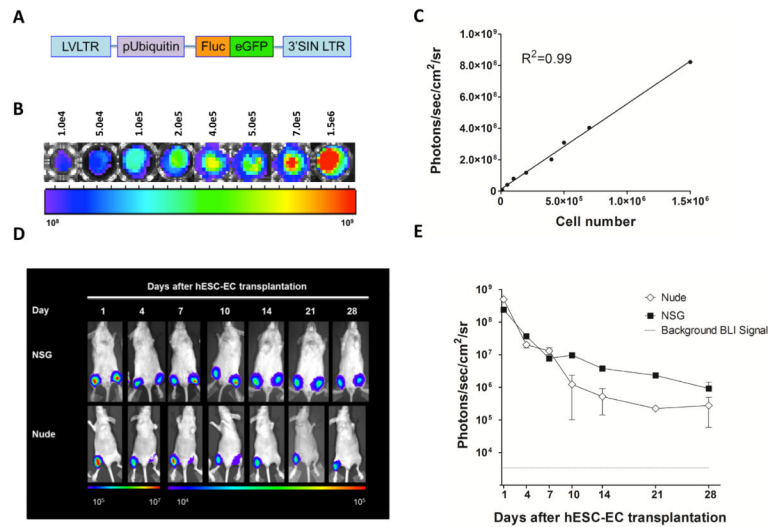


Figure 2. hESC-EC transplantation and survival in immunodeficient hosts. **(A)** Schematic of double fusion reporter gene construct with a constitutive human ubiquitin promoter driving expression of Fluc and eGFP, with a self-inactivating (SIN) lentiviral vector. **(B, C)** Correlation of cell count with Fluc signal ($R^2 = 0.99$). **(D)** Strong cell engraftment after hindlimb transplantation in immunodeficient NOD scid gamma (NSG) and Nude mice. **(E)** BLI signal quantification of panel D.

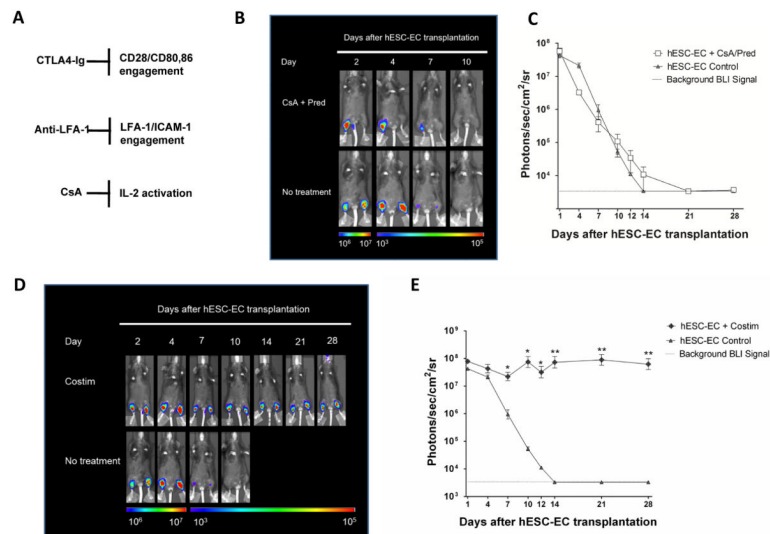


Figure 3. Costimulation-adhesion therapy (Costim) is superior to cyclosporine (CsA) and prednisone therapy in promoting hESC-EC survival. **(A)** CTLA4-Ig competes with CD28 for CD80/86 binding; anti-LFA-1 inhibits LFA-1/CAM-1 interaction; and CsA blocks production of IL-2. **(B)** Cell survival is limited in immunocompetent animals and is not significantly improved by CsA/Pred therapy. **(C)** BLI signal quantification of panel B. **(D)** Costimulation-adhesion therapy significantly improves hESC-EC survival compared to no treatment. **(E)** BLI signal quantification of panel D (* $p < 0.05$; ** $p < 0.01$).

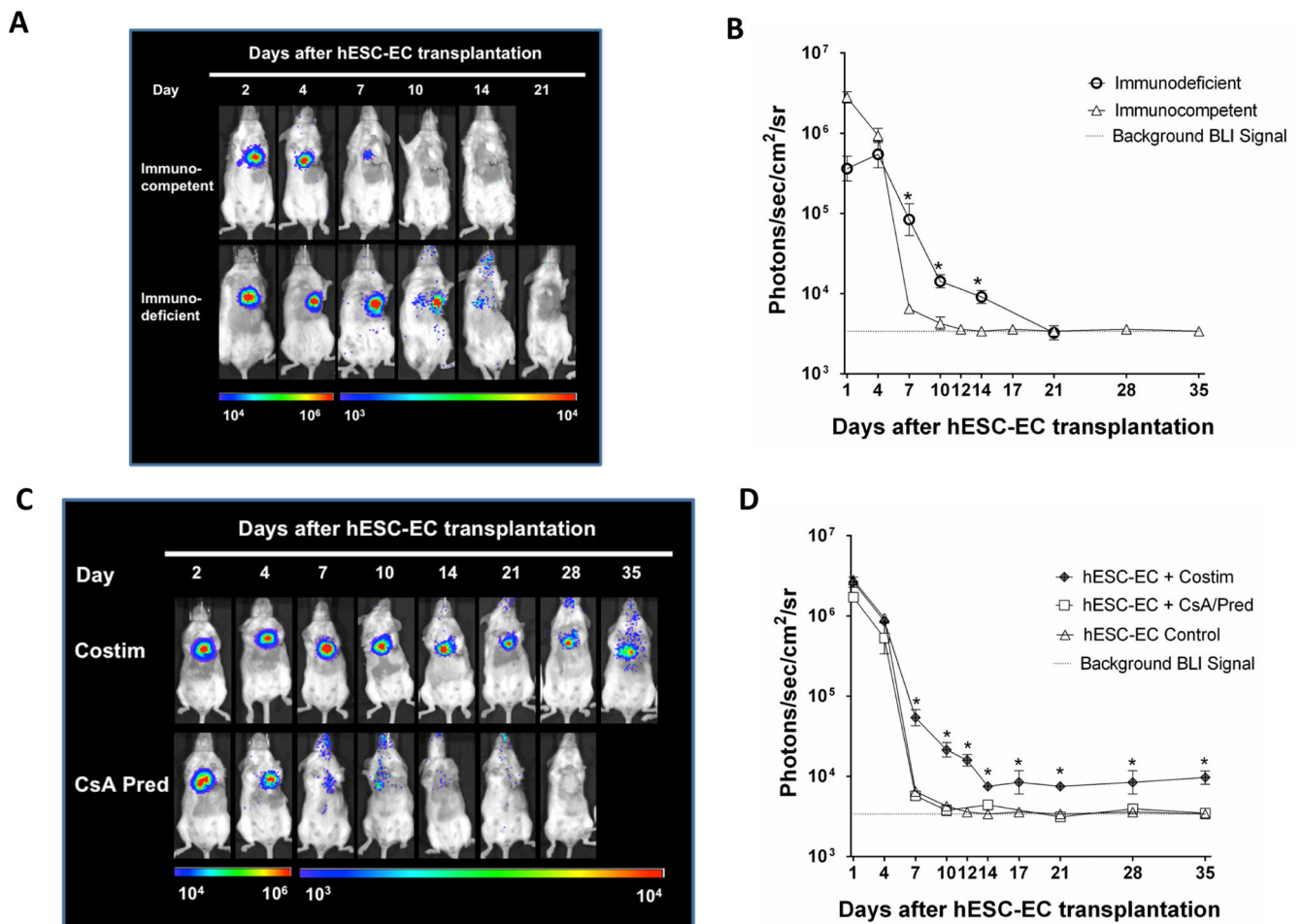


Figure 4. Costimulation-adhesion therapy promotes survival and engraftment of hESC-ECs in a myocardial infarction model. **(A)** Superior hESC-EC engraftment in immunodeficient (NOD/SCID) compared to immunocompetent (FVB) animals. Survival of hESC-ECs in immunocompetent mice was limited by day 10 whereas hESC-ECs in immunodeficient SCID mice engrafted up to day 21. **(B)** BLI signal quantification of panel A ($*p < 0.05$). **(C)** Costimulation-adhesion therapy (costim) permits the strong engraftment of hESC-ECs compared to mice receiving CsA/Pred therapy. **(D)** BLI signal quantification of panel C ($*p < 0.05$ costim compared to immunocompetent control, and costim compared to CsA/Pred).

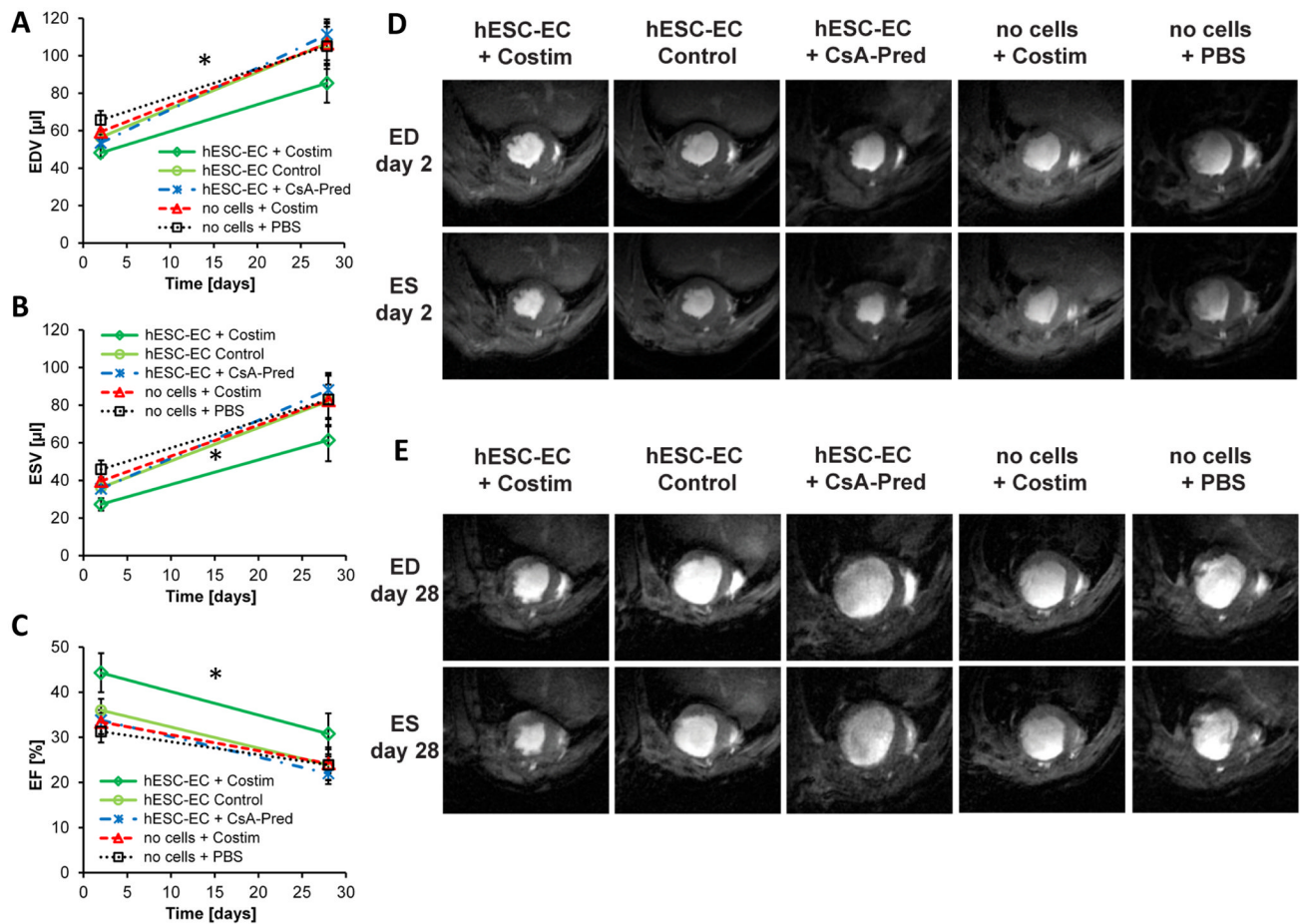
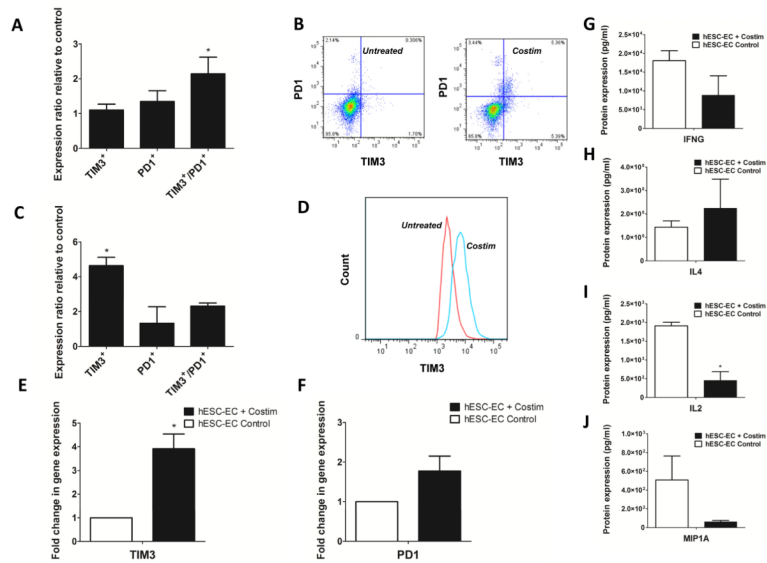


Figure 5.

Animals treated with costimulation-adhesion therapy and hESC-ECs showed improved cardiac function following myocardial infarction. (A–C) MRI analyses with plots for end diastolic volume (EDV), end systolic volume (ESV), and ejection fraction (EF) of animals with either (1) hESC-ECs + costimulation-adhesion therapy (costim); (2) hESC-ECs + no treatment; (3) hESC-ECs + CsA/Pred; (4) no cells + costim; or (5) no cells + PBS at day 2 and day 28 after MI (n=6–9/group). EDV and ESV were significantly lower and EF was significantly higher in animals treated with hESC-ECs and costimulation-adhesion agents compared to all other groups (ANOVA, $*p < 0.05$ hESC-ECs + costim compared to all other groups), indicative of reduced remodeling and increased cardiac function. (D, E) Representative short-axis images of infarcted hearts at 2 days and 28 days after surgery of animals with (1) hESC-ECs + costim; (2) hESC-ECs + no treatment; (3) hESC-ECs + CsA/Pred; (4) no cells + costim, or (5) no cells + PBS. Scale bars = 5 mm; width of individual cardiac images = 18 mm.

**Figure 6.**

Improved hESC-EC engraftment by costimulation-adhesion therapy is associated with upregulation of TIM3 and downregulation of a pro-inflammatory cytokine profile. **(A, B)** Marked increase in TIM3⁺PD1⁺ cells in splenocytes of costimulation-adhesion treated animals compared to untreated controls ($*p < 0.05$). **(C, D)** Significant upregulation of TIM3⁺ cells in hindlimb muscle tissue implanted with hESC-ECs harvested from costimulation-adhesion-treated animals compared to untreated controls ($*p < 0.05$). **(E, F)** RT-PCR of lymph node cells from costimulation-adhesion-treated animals also reveals upregulation of TIM3 and PD1 compared to untreated control animals. **(G–J)** Downregulation of IL-2, IFN- γ , and MIP1- α , and upregulation of IL-4 in splenocytes of costimulation-adhesion-treated animals compared to controls ($*p < 0.05$, only in IL-2).